GEOPHYSICS, VOL. 70, NO. 1 (JANUARY-FEBRUARY 2005); P. V10–V20, 15 FIGS.
10.1190/1.1852789

Multiple attenuation in the image space

Paul Sava[1] and Antoine Guitton[1]

ABSTRACT

Multiples can be suppressed in the angle-domain image space after migration. For a given velocity model, primaries and multiples have different angle-domain moveout and, therefore, can be separated using techniques similar to the ones employed in the data space prior to migration. We use Radon transforms in the image space to discriminate between primaries and multiples and employ accurate functions describing angle-domain moveouts. Since every individual angle-domain common-image gather incorporates complex 3D propagation effects, our method has the advantage of working with 3D data and complicated geology. Therefore, our method offers an alternative to the more expensive surface-related multiple-elimination (SRME) approach operating in the data space.

Radon transforms are cheap but not necessarily ideal for separating primaries and multiples, particularly at small angles where the moveout discrepancy between the two kinds of events are not large. Better techniques involving signal/noise separation using prediction-error filters can be employed as well, although such approaches fall outside the scope of this paper. We demonstrate, using synthetic and real data examples, the power of our method in discriminating between primaries and multiples after migration by wavefield extrapolation, followed by transformation to the angle domain.

INTRODUCTION

The current most robust multiple-attenuation techniques exploit moveout discrepancies between primaries and multiples (Foster and Mosher, 1992). For instance, for relatively simple geology, normal-moveout (NMO) correction efficiently flattens the primaries and leaves the multiples curved. Then the primaries and multiples can be separated in the Radon domain. However, it has been recognized that NMO and Radon transforms are not optimal when complex wavefield propagation occurs in the subsurface, mainly because the moveout of primaries and multiples can no longer be described with simple functions (parabolic or hyperbolic) in such situations (Bishop et al., 2001). Therefore, more sophisticated methods are needed to perform the multiple attenuation.

One method that takes propagation effects into account is the surface-related multiple-attenuation (SRME) approach (Verschuur et al., 1992). This technique has the advantage of working with the surface data only and for any type of geology. Thus, it is often the method of choice for multiple attenuation in complex geology (Miley et al., 2001). To be accurate, the SRME method requires dense coverage of sources and receivers. Whereas this condition is relatively easy to meet in 2D, it becomes much more difficult to fulfill with 3D surveys; therefore, new multiple-prediction techniques are developed to circumvent this limitation (van Dedem and Verschuur, 2001; Levin and Johnston, 2001).

A powerful multiple-attenuation technique would be one that first takes the wavefield propagation into account and then uses moveout discrepancies to remove multiples. To achieve this goal, we propose using prestack depth migration as our imaging operator instead of NMO. Assuming that we have a reasonable velocity model and an accurate migration scheme, we can then image complex geology very accurately. In this process, *both* primaries and multiples are migrated, after which they are transformed to angle gathers using standard techniques. In the angle domain, primaries are flat and multiples are curved, mimicking the situation we have after NMO for simple geology. Finally, we propose mapping the angle gathers into a Radon domain where the signal/noise separation can be achieved.

Our method has the potential to work with 2D or 3D data as long as angle gathers can be estimated correctly and moveout separation between primaries and multiples can be achieved. It is also much cheaper than the SRME approach, but it can still handle complicated geologic media, since propagation is described by accurate wavefield extrapolation operators.

Manuscript received by the Editor July 25, 2003; revised manuscript received July 15, 2004; published online January 14, 2005.
[1]Stanford University, Geophysics Department, Stanford Exploration Project, Mitchell Building, Stanford, California 94305-2215. E-mail: paul.sava@stanford.edu; antoine@sep.stanford.edu.

An approach similar to ours is used by Duquet and Marfurt (1999) to discriminate coherent noise in offset gathers during and after Kirchhoff migration. In contrast, we use angle gathers and migration by wavefield extrapolation (WE) instead of offset gathers and Kirchhoff migration. The main reasons for our choices are: (1) images obtained by WE migration in complicated areas, e.g., under salt, are of better quality with fewer artifacts, since all multiple arrivals are employed in imaging, and (2) angle gathers are single valued even when created with incorrect velocity, in contrast to offset gathers, which are not (Stolk and Symes, 2002). A drawback of the angle domain is that angular coverage decreases significantly with depth, which makes event discrimination based on moveout harder.

In the following section, we briefly review the transformation from offset to angle with WE migration. Then we present our multiple-attenuation strategy with angle-domain Radon transforms. Finally, we illustrate the proposed method with synthetic and field datasets. We show that multiple attenuation in the image space considerably improves the migrated images.

ANGLE TRANSFORM

Angle-domain common-image gathers (ADCIGs) are decompositions of seismic images in components proportional to the reflection magnitude for various incidence angles at the reflector (Figure 1). Given correct velocities and migration algorithms, primaries map into flat gathers, and multiples map into events with moveout.

Angle gathers can be constructed by two classes of methods: data-space methods (de Bruin et al., 1990; Prucha et al., 1999; Mosher and Foster, 2000), with reflectivity described as a function of offset ray parameter p_h:

$$\rho_h = \frac{\partial t}{\partial h}|_{z,x}, \tag{1}$$

and image-space methods (Weglein and Stolt, 1999; Sava and Fomel, 2003), with reflectivity described as a function of scattering angle γ:

$$\tan\gamma = -\left.\frac{\partial z}{\partial h}\right|_{t,x}, \tag{2}$$

where t represents time, z and x stand for the depth and location of the reflection point, and h represents the offset at depth after downward continuation (Figure 1). Both transformations in equations 1 and 2 are slant stacks in the space/time domain, or radial trace transforms in the Fourier domain. Three-dimensional extensions of these transformations are presented by Biondi et al. (2003).

Hereafter, we will not distinguish between the two kinds of ADCIGs, since the moveout behavior of primaries and multiples are similar, irrespective of the method we use. For all examples, however, we use the image-space method, which outputs reflectivity as a function of scattering angle at the reflector.

Angle-domain common-image gathers are useful for multiple suppression for several reasons. First, events imaged with the wrong velocity show substantial moveout, which allows us to discriminate between primaries imaged with correct velocity, and multiples imaged with incorrect velocity. Second, ADCIGs describe the reflectivity at the reflection point, independent, in principle, from the actual structure for which they are computed, so they capture all 3D propagation effects at every individual CIG. Finally, multiple attenuation in the image space gives us the opportunity to directly appraise the impact of our multiple processing in the final image. Therefore, we can more easily surgically remove, or mute, multiples in areas of interest and with more control of the final result.

Among the difficulties associated with angle gathers are the reduced angular coverage and illumination gaps in subsalt areas. In such cases, either the events mapped with incorrect velocity (multiples) do not show enough separation from events mapped with correct velocity (primaries), or the two types of events are obscured by truncation artifacts, making it more difficult to separate signal from noise with Radon transforms.

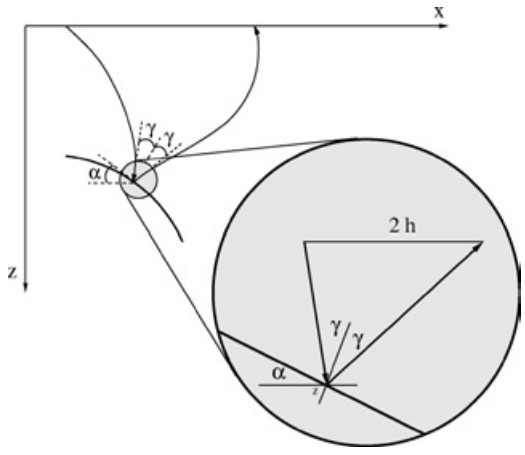

Figure 1. Reflection rays in an arbitrary-velocity medium: α is the reflector dip angle, γ is the reflection angle measured relative to the normal to the reflector, h is the offset at depth after downward continuation, and z and γ are the depth and location of the reflection point.

MULTIPLE SUPPRESSION

Multiple-attenuation methods using Radon transforms (RT) are popular and robust (Foster and Mosher, 1992). These techniques use the moveout discrepancies between primaries and multiples for discrimination. Usually, the multiple attenuation is carried out with common-midpoint (CMP) gathers after NMO correction (Kabir and Marfurt, 1999). Then, the corrected data are mapped with a parabolic Radon transform (PRT) into a domain where primaries and multiples are separable.

One desirable property of a Radon transform is that events in the Radon domain are well focused, i.e., sparse. This property makes the signal/noise separation much easier and decreases the transformation artifacts. These artifacts come, essentially, from the null space associated with the RTs (Thorson and Claerbout, 1985). The RTs can be made sparse in the Fourier domain (Hugonnet et al., 2001) or in the time domain (Sacchi and Ulrych, 1995). The Fourier-domain approach has the advantage of allowing fast computation of the Radon panel (Kostov, 1990), although the sparse condition developed to date (Hugonnet et al., 2001) does not focus the

energy in the time axis. Therefore, in our implementation of the RTs, we opted for a time-domain formulation with a Cauchy regularization in order to enforce sparseness in both time and space.

A generic equation for a Radon transform in the angle domain is

$$z(q,\gamma) = z_0 + q\ g(\gamma), \tag{3}$$

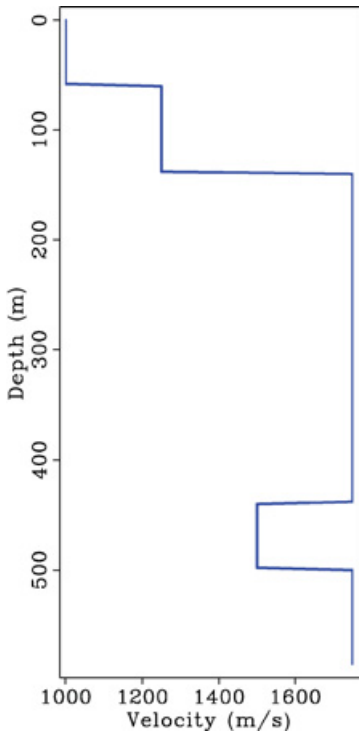

Figure 2. Simple synthetic model; v(z) velocity function used for 2D finite-difference modeling. The bottom of the model is a reflecting boundary.

where z_0 is the zero-angle depth, γ is the scattering angle, q is a curvature parameter, and $g(\gamma)$ is a function that represents the moveout in the CIGs. The modeling equation from the Radon domain to the image domain and its adjoint are

$$d(z,\gamma) = \sum_{z_0}\sum_{q} m(z_0,q)\delta\{z_0 - [z - q\ g(\gamma)]\}, \tag{4}$$

$$m(z_0,q) = \sum_{z}\sum_{\gamma} d(z,\gamma)\delta\{z - [z_0 + q\ g(\gamma)]\}, \tag{5}$$

where $d(z,\gamma)$ is the data represented by CIGs in the angle domain, and $m(z_0,q)$ is the model represented by the CIGs transformed to the Radon domain. At first order, we can assume that $g(\gamma) = \gamma^2$, which shows that equation 3 corresponds to the definition of a parabola. However, for ADCIGs, Biondi and Symes (2004) demonstrate that, in the absence of structural dip, a better approximation is $g(\gamma) = tan^2(\gamma)$.

Equation 4 can also be written in matrix form as

$$\mathbf{d} = \mathbf{Lm}, \tag{6}$$

where $\mathbf{d}$ is the image in the angle domain, $\mathbf{m}$ is the image in the Radon domain, and $\mathbf{L}$ is the forward RT operator. Our goal now is to find the vector $\mathbf{m}$ that best synthesizes, in a least-squares sense, the data $\mathbf{d}$ by the operator $\mathbf{L}$. Therefore, we want to minimize the objective function:

$$f(\mathbf{m}) = \|\mathbf{Lm} - \mathbf{d}\|^2. \tag{7}$$

We also add a regularization term that enforces sparseness in the model space $\mathbf{m}$. High resolution can be obtained by imposing a Cauchy distribution in the model space (Sacchi and Ulrych, 1995):

$$f(\mathbf{m}) = \|\mathbf{Lm} - \mathbf{d}\|^2 + \epsilon^2 b^2 \sum_{i=1}^{n} ln\left(1 + \frac{m_i^2}{b^2}\right), \tag{8}$$

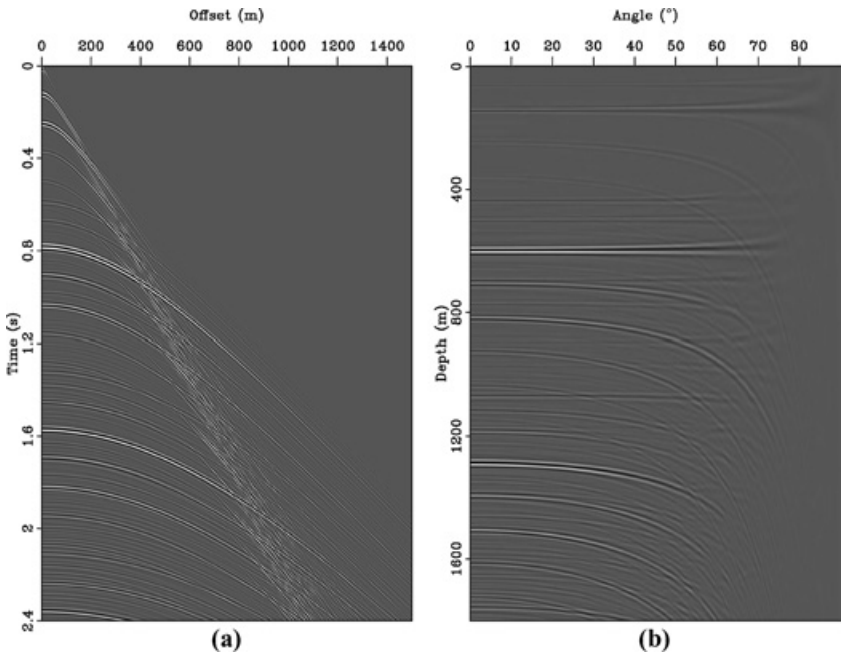

Figure 3. Simple synthetic model; (a) A data-space CMP and (b) a corresponding image-space CIG.

where n is the size of the model space, and ε, b are two constants chosen a priori: ϵ controls the amount of sparseness in the model space, and b relates to the minimum value below which everything in the Radon domain should be zeroed. The least-squares inverse of $\mathbf{m}$ is

$$\hat{\mathbf{m}} = \left[\mathbf{L}'\mathbf{L} + \epsilon^2 \mathbf{diag}\left(\frac{1}{1+\frac{m_i^2}{b^2}}\right)\right]^{-1} \mathbf{L}'\mathbf{d}, \qquad (9)$$

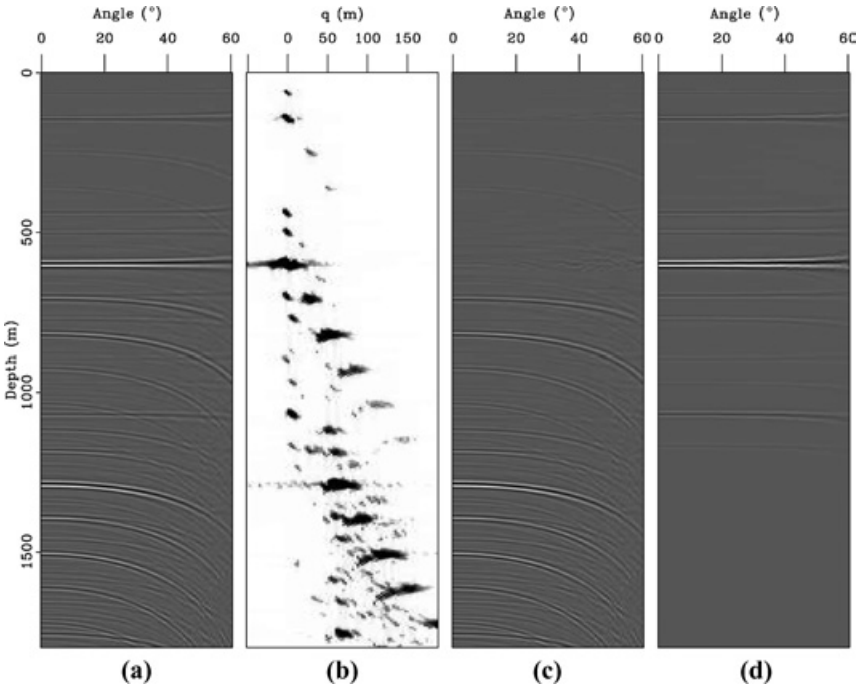

Figure 4. Synthetic example for signal/noise separation in the image space. (a) Data in the image domain, (b) data in the Radon domain, (c) multiples (noise), and (d) primaries (signal).

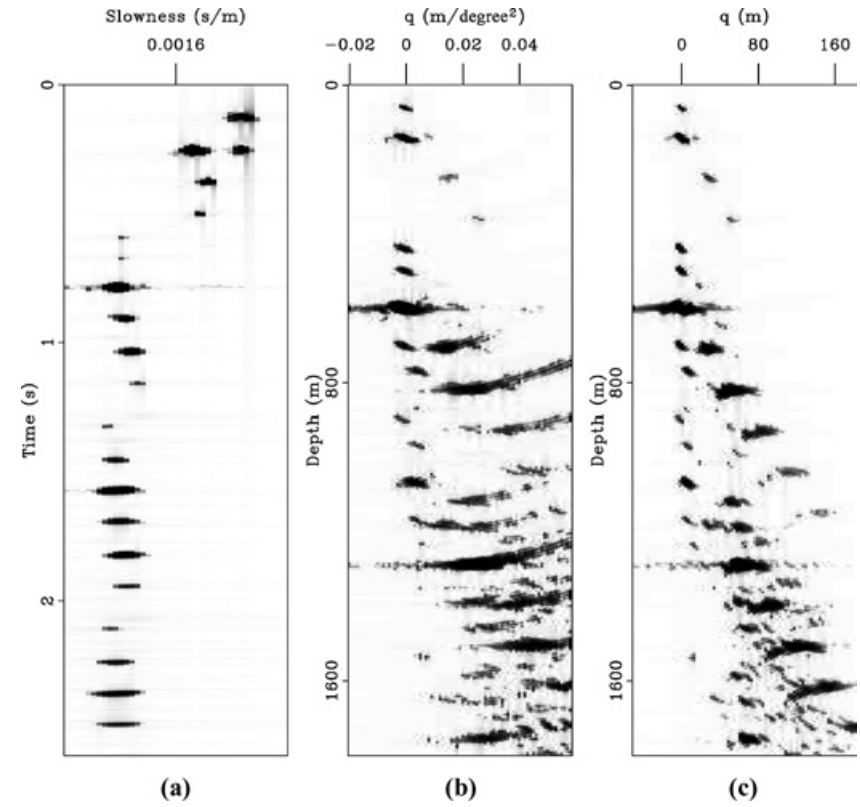

Figure 5. Radon transform of the data in Figure 3. (a) Hyperbolic Radon transform in the data space, (b) Radon transform in the angle domain using the parabolic equation, and (c) the tangent equation.

where **diag** defines a diagonal operator. Because the model or data space can be large and the objective function nonlinear, we estimate **m** iteratively. The objective function in equation 8 is nonlinear because the model appears in the definition of the regularization term. Therefore, we use a limited-memory quasi-Newton method (Guitton and Symes, 2003) to find the minimum of $f(\mathbf{m})$.

From the estimated model **m**, we separate multiples from primaries in the Radon domain, using their distinct q values. We transform the multiples back to the image domain by applying **L** and subtract them from the input data to obtain multiple-free angle gathers.

EXAMPLES

Our first example corresponds to a synthetic model with flat reflectors and $v(z)$ velocity (Figure 2). We use this example to illustrate the main features of our method, although this situation is simple enough to be handled by NMO and RT in the data space. The left panel in Figure 3 is a representative

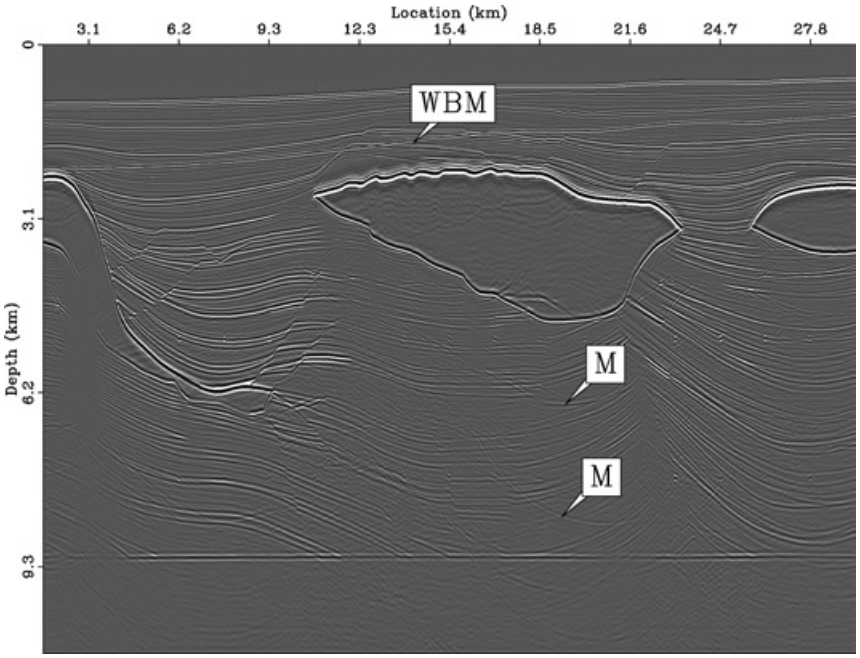

Figure 6. Smaart JV Pluto synthetic model. Migrated image without multiple suppression. WBM shows the strong, first-order, water-bottom multiple. The two Ms point to weaker surface-related multiples linked to the salt body.

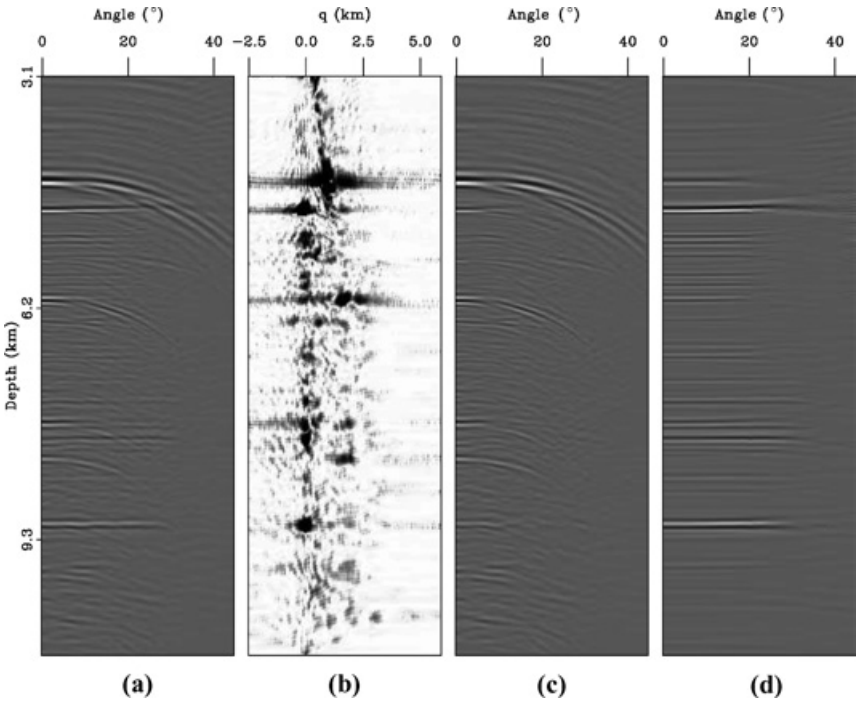

Figure 7. Smaart JV Pluto synthetic model. Signal/noise separation in the image space. (a) Primaries + multiples (data), (b) data in the Radon domain, (c) multiples (noise), and (d) primaries (signal).

CMP for this model, in which most of the energy is multiples. The right panel in Figure 3 depicts a corresponding CIG. Again, most of the energy in the gather is multiples, which have nonflat moveout that distinguishes them from the flat primaries.

Figure 4 shows, from left to right: (a) the data equal the primaries plus multiples in the image space; (b) the data transformed to the Radon domain, where the flat primaries are represented in the vicinity of $q = 0$, in contrast to the multiples at nonzero q; (c) the multiples isolated in the Radon domain and transformed back to the image domain; and (d) the primaries left after subtraction of the multiples (c) from the data (a).

Figure 5 shows a comparison between hyperbolic Radon transform (HRT) in the data space and Radon transforms in the image space using the parabolic equation $g(\gamma) = \gamma^2$, and the more accurate tangent equation $g(\gamma) = tan^2(\gamma)$. Although HRT focuses all events very well in this simple velocity model, creating a mute function that separates primaries from multiples remains an interpretation challenge. In contrast, the Radon transforms in the image space focus all primary energy at $q = 0$; therefore, it is much easier to design an appropriate mute function. Furthermore, we observe better focusing using the tangent equation, which makes multiples easier to separate from primaries.

Next, we illustrate our method with the Smaart JV Pluto synthetic model. The migration result with the correct velocity is shown in Figure 6. Note that the surface-related multiples do not create strong imaging artifacts below the salt body and that the image is interpretable overall. In Figure 6, WBM shows the location of the migrated water-bottom multiple. This event is by far the strongest multiple. The two Ms point to relatively strong subsalt multiples. Figure 7 shows our processing on one CIG at $x = 18.5$ km, following the pattern used in the preceding example. Flat events are very well separated.

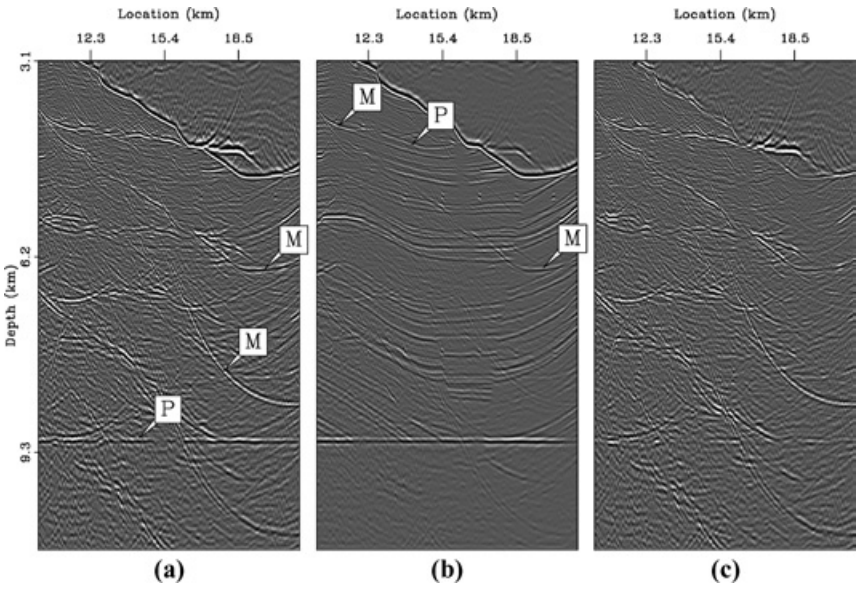

Figure 8. Smaart JV Pluto synthetic model. Common-angle sections (CAS) at scattering angle $\gamma = 0^\circ$. (a) CAS of primaries + multiples (data). P is a flat primary obscured by multiples. Ms are two strong salt-related multiples. This panel shows many strong artifacts caused by the multiples. (b) CAS of primaries (signal) separated in the image space. The multiples (M) are very well attenuated and only a few remain. P points to primary events that were not visible in (a). (c) CAS of multiples = data (a)–primaries (b).

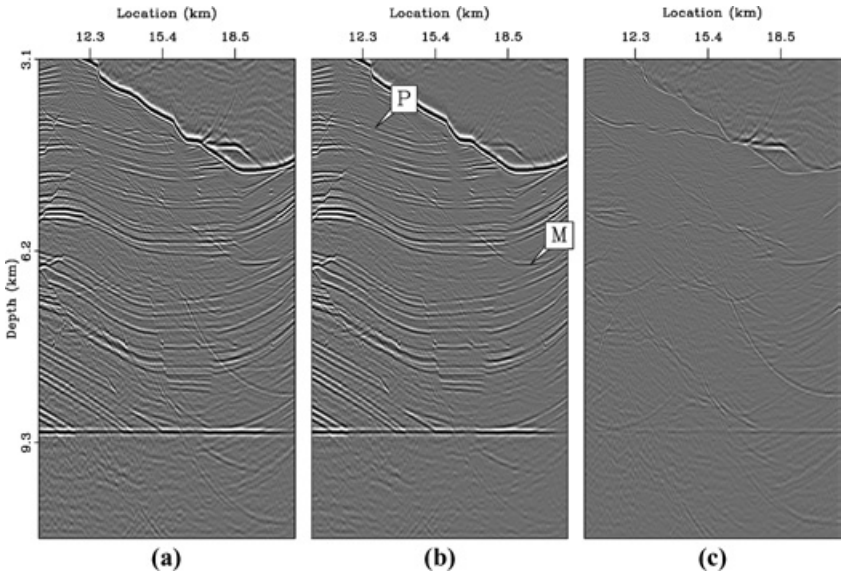

Figure 9. Smaart JV Pluto synthetic model. Stacked sections. (a) Stack of primaries + multiples (data). The stack greatly reduces the multiple energy. (b) Stack of primaries (signal) separated in the image space. Although cleaner than in (a), some multiple energy (M) remains. P points to a cleaner reflector. (c) Stack of multiples = data (a)–primaries (b).

Figure 8 shows a comparison of common-angle sections at 0° scattering angle of the data before multiple suppression, after multiple suppression, and of the estimated multiples. The artifacts caused by the multiples in Figure 8a are very strong. For example, the flat reflector P at 9.3 km is well attenuated. The two multiples shown as M in Figure 8a are almost completely removed in Figure 8b. The two remaining multiples M in Figure 8b are almost flat in the angle domain; therefore, their attenuation is difficult to achieve. Nevertheless, the overall attenuation result is pleasing, since most of the multiples are removed while preserving the primaries (Figure 8c).

Figure 9 shows a comparison of stacked images across angles for the data, the estimated primaries, and the estimated multiples. The stack of the data in Figure 9a greatly reduces the multiples. Our multiple-attenuation scheme eliminates much of the multiple energy (P in Figure 9b). The multiple event M in Figure 9b does not stack out very well; it remains after our multiple removal technique because its moveout is almost flat in the angle domain. As seen in Figure 9c, most of the multiple energy is removed from the image, although a small amount of residual multiples is left behind. From this example, we can conclude that our multiple attenuation in the image space works well in complex geology. Although not

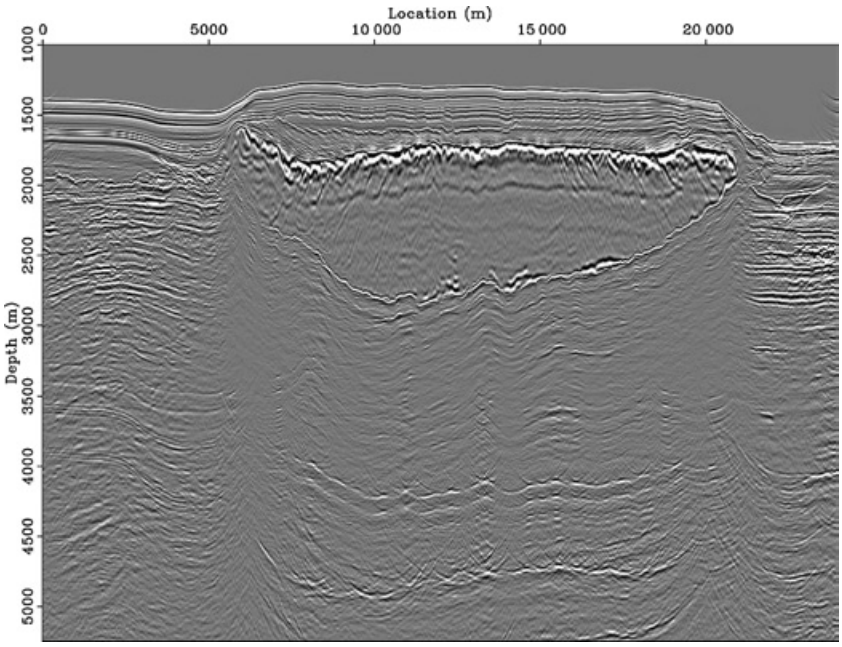

Figure 10. Gulf of Mexico example. Migrated image without multiple suppression. The salt body generates strong reverberations that are migrated below 3000 m.

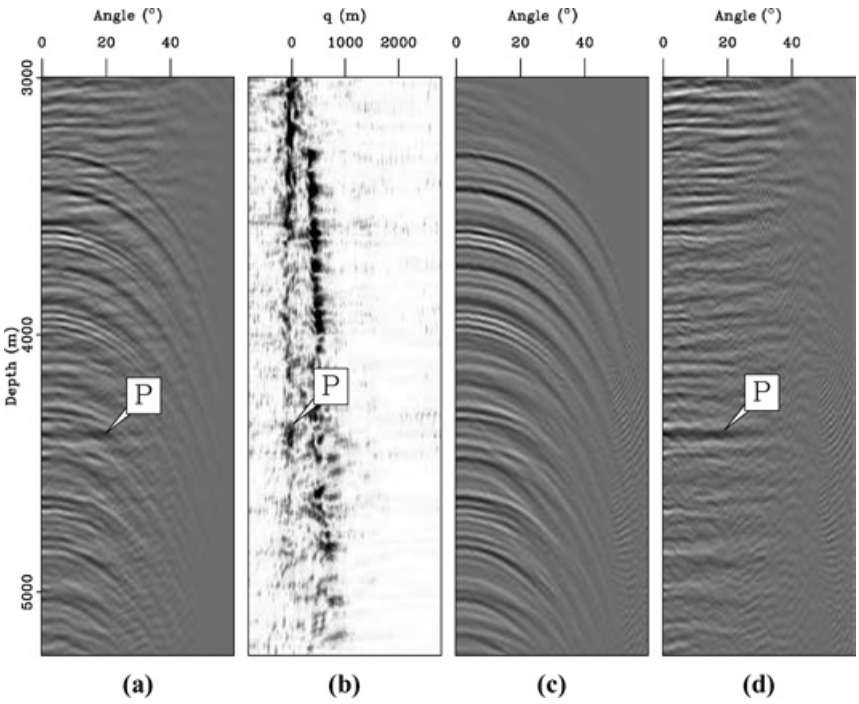

Figure 11. Gulf of Mexico example. Signal/noise separation in the image space at $x = 2000$ m. (a) Primaries + multiples (data). P points to a primary embedded in the multiples. (b) Data in the Radon domain. Primaries (leftmost corridor) and multiples (rightmost) are well separated. P shows the location in the Radon domain of the primary in (a). (c) Multiples (noise). (d) Primaries (signal). The primary event at P is recovered.

perfect, the removal of multiples in the image space has the advantage of (1) cleaning up the angle gathers very well, thus allowing a better interpretation of the amplitude-versus-angle (AVA) responses, and (2) providing better migrated images for structural interpretation.

We also apply our technique to a Gulf of Mexico dataset from a salt dome environment. Figure 10 shows the migrated image without multiple suppression. The surface-related multiples are easily seen below 3000 m. The shallow salt body generates most of these multiples. In addition to these events, 3D/out-of-plane multiples are also present, making 2D SRME less efficient. This is a more complicated example, since it illustrates many of the difficulties encountered by multiple suppression in complicated areas, around salt bodies, and in the presence of notable 3D effects. In addition, our velocity model is certainly not exact, making the moveout analysis in the angle domain more challenging.

Following the pattern used in the preceding example, Figures 11 and 12 show our multiple analysis at two different locations in the data. Figure 11 corresponds to an area away from the salt body ($x = 2000$ m). Figure 11b illustrates the clear separation between the multiple trend on the left and the primary trend on the right. P denotes a primary hidden in the multiples. This event is well recovered after muting,

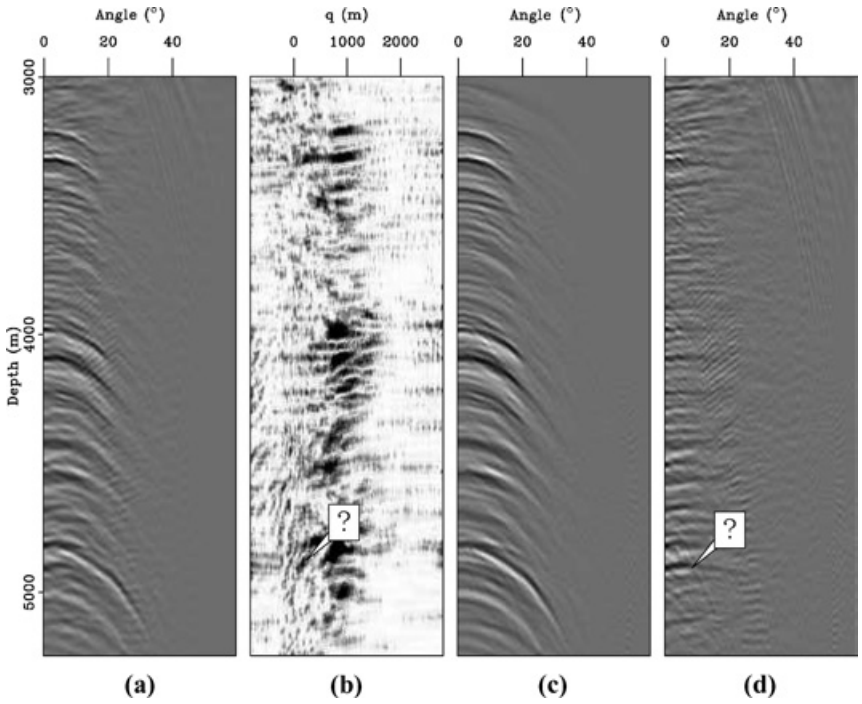

Figure 12. Gulf of Mexico example. Signal/noise separation in the image space at $x = 8000$ m. The events shown are subsalt with a limited angle coverage. (a) Primaries + multiples (data). It is almost impossible to distinguish any primary. (b) Data in the Radon domain. The arrow points to an event that might be a primary. (c) Multiples (noise). (d) Primaries (signal). The suspected primary is separated, but it remains difficult to know if this event corresponds to a real reflector.

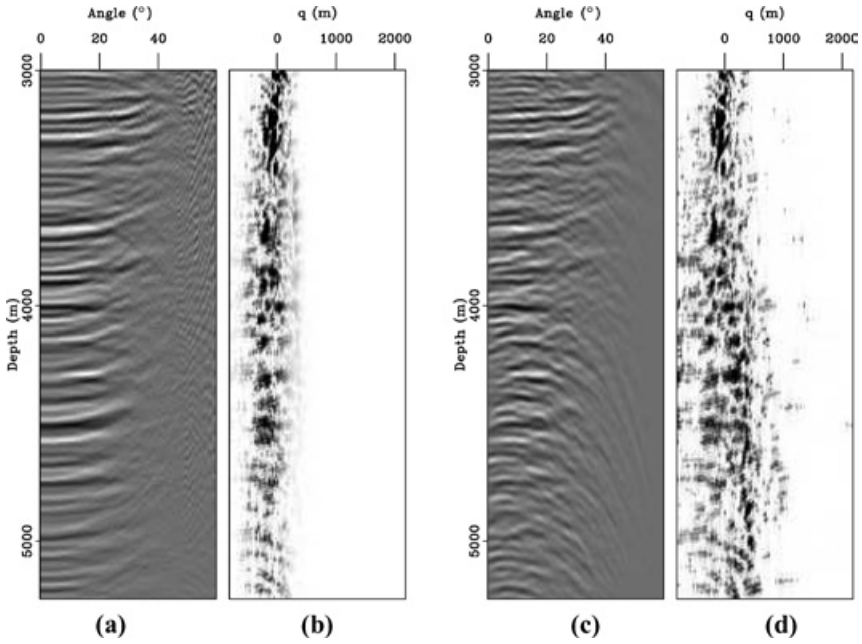

Figure 13. Gulf of Mexico example. CIG at $x = 3000$ m. (a) CIG of primaries after multiple suppression in the image space. (b) Radon transform of the data in panel. (a). (c) CIG of primaries after multiple suppression in the data space. (d) Radon transform of the data in panel (c).

as shown in Figure 11d. In addition, the estimated primaries are not exactly flat in the angle domain, thus proving that the velocity we used is not correct. Figure 12 corresponds to a region directly under the salt ($x = 8000$ m). In this area, it is very difficult to see any primary at all. The arrows in Figures 12b and d show an event that might be a primary. In Figure 12b, focusing and separation of the different events are not as good as in Figure 11b. Our interpretation is that we have neither the right velocity model nor a perfect representation of the moveout in this complex environment. In addition, the angle coverage under the salt in Figure 12a is smaller than the angle coverage outside the salt boundaries in Figure 11a. This short-angle coverage can degrade focusing of the primaries in the Radon domain, thus making the separation more difficult to achieve. Although not an issue with this dataset, the ability to focus events should always be assessed in complex geology.

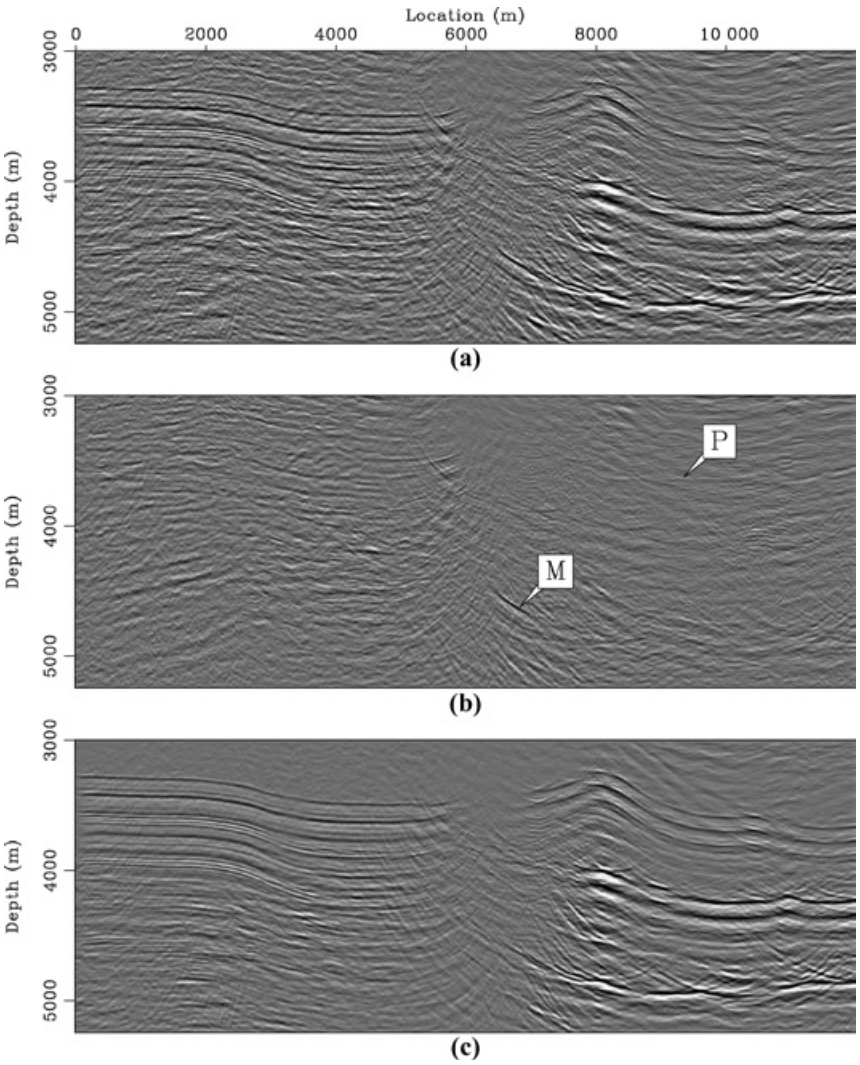

Figure 14. Gulf of Mexico example. Common-angle sections (CAS) at scattering angle $\gamma = 10^\circ$. (a) CAS of primaries + multiples (data). (b) CAS of primaries (signal) separated in the image space. M shows a multiple that stays in the image after separation. P points to an event that seems to be unraveled by our separation. (c) CAS of multiples = data (a)–primaries (b). Most of the events caused by the multiples are well attenuated.

For comparison, Figure 13 shows a CIG at $x = 3000$ m after multiple suppression in the image space and after multiple suppression in the data space using a high-resolution HRT with Cauchy regularization, as well as the angle-domain Radon transforms of these images. We observe that multiple suppression in the image space creates significantly cleaner image gathers with fewer residual multiples, as illustrated by the smaller amount of energy in the Radon domain away from $q = 0$.

Figure 14 shows a comparison of common-angle sections at 10° of the data before multiple suppression, the estimated primaries, and the estimated multiples. Much of the multiple energy has been attenuated, and a primary seems to appear at P (Figure 14b). In contrast, a strong multiple, M, at the edge of the salt, has not been attenuated at all. In this area of poor illumination, our method failed. As a final result, Figure 15 shows a comparison of stacked images across angle for the data, the primaries, and the multiples. Note that we stacked from 7° and above, thus removing short-angle artifacts of the Radon transform. Figure 15b proves that our method significantly reduces the multiple energy in the final image while preserving the primaries (see Figure 15c): the P event in Figure 15b seems to be well imaged. As previously noted for Figure 14b, the strong multiple M at the salt edge is not well attenuated.

DISCUSSION

Primaries and multiples can have shapes in the data space that are neither parabolic nor hyperbolic. All multiple suppression strategies based on PRT, HRT, or similar methods approximate the data moveout and may fail in complex areas. Furthermore, primaries and multiples often have comparable shapes that are hard to discriminate.

In contrast, primaries in the angle-domain image space are mostly flat, while multiples are not. This allows, in principle, for good discrimination between the two kinds of events using robust signal/noise-separation strategies. However, as with data-space methods, it is difficult to separate primaries and multiples using Radon transforms if they do not have a clear separation (e.g., small reflection angles).

For complex geology, multiples are better attenuated if the propagation effects are taken into account. This is why the SRME approach performs so well (Verschuur et al., 1992). For 3D data, the latter can be rather difficult to use because of the considerable expense of acquiring dense 3D data and/or interpolating the sources and receivers on a regular grid. Alternatively, we can migrate the data and do the separation in the image space with conventional Radon transforms, as we demonstrate in this paper.

In a generic way, SRME employs the entire wavefield (data) to predict where multiples occur, and then subtracts them using various procedures. Therefore, we can look at SRME as a method employing (full-wavefield) prediction followed by subtraction. Our method operates similarly, by mapping the data in the image space (prediction) using a full-wavefield operator (wave-equation migration), followed by subtraction after Radon transform.

Potential pitfalls for the multiple-suppression strategy in the image space include situations where our velocity model is growly inaccurate. We encounter the theoretical possibility that some multiples are flat (focused) and some primaries are not flat (unfocused). Both types of events leak in the Radon domain in the space where we would normally encounter the other type of event, and it is harder to see the separation needed to discriminate primaries from multiples. However, if the velocity model is more or less correct, we can still discriminate primaries from multiples, given enough separation in the Radon domain. Our Gulf of Mexico example illustrates this, since the velocity model under salt represents a lateral extension of a $v(z)$ model estimated away from salt.

If the migration algorithm is implemented correctly, and if the velocity model is more or less correct, the primaries map to approximately flat events. Multiples, on the other hand, can have complicated moveouts, which is particularly true for diffracted multiples. Nevertheless, since one of the events we are trying to distinguish is simple (flat primaries), we have a better chance to separate events in the image space than in the data space, where both primaries and multiples can have complicated moveouts. However, the angle domain is not 100% failproof either, since both primaries and multiples can be complicated by illumination. In such cases, some portion of the primary events are missing and we observe truncation "smiles," which can complicate the moveouts considerably. This limitation is also common for migration velocity analysis.

Finally, we would like to point out that the strategy described in this paper is not ideal. One of the known drawbacks of multiple suppression using Radon transforms is the overlap of some of the multiple energy maps at the origin of the transform axis (scattering angle, in our case) with the primaries. Consequently, some multiple energy remains in the final image, regardless of the accuracy of the mute function. Other, more sophisticated signal/noise-separation methods, e.g., those based on patterns (Guitton et al., 2001), can better handle the nonparabolic shapes encountered in the image space, thus producing better separation results. The primaries and multiples separated by Radon transforms in the image space can serve as the training objects on which we can define the prediction-error filters used for pattern-based separation, similar to the procedure employed by SRME in the data space.

CONCLUSIONS

Multiples can be suppressed in the angle domain after migration. For a given velocity model, primaries and multiples have different moveout in the image space; therefore, they can be separated using techniques similar to the ones employed in the data space prior to migration. We use Radon transforms, although these methods are neither unique nor ideal.

Because we are using prestack depth migration, this method takes into account the effects of complex wavefield propagation in the same way that the SRME approach does. However, our proposed scheme has the potential to be more affordable with 3D data. For complex geology, our method stands

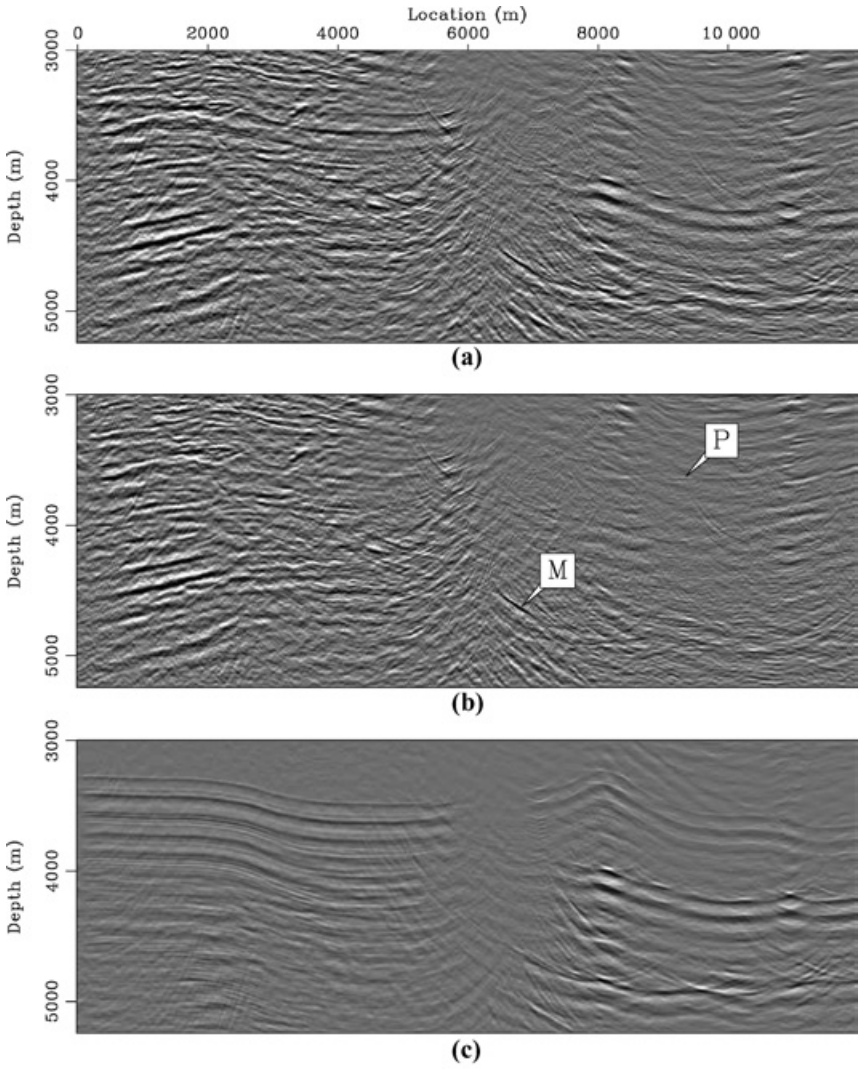

Figure 15. Gulf of Mexico example. Stacked sections. (a) Stack of primaries + multiples (data). (b) Stack of primaries (signal) separated in the image space. M shows a multiple that stays in the image after separation. P points to an event that seems to be unraveled by our separation. (c) Stack of multiples = data (a)–primaries (b). Most of the events caused by the multiples are well attenuated.

between multiple attenuation in the data space with Radon transforms (inaccurate, but cheap and robust), and the SRME approach, where multiples are first predicted and then subtracted (accurate, but expensive).

ACKNOWLEDGMENTS

We would like to thank Biondo Biondi of Stanford University for useful suggestions. We would also like to acknowledge the associate editor, Eric Verschuur, and three anonymous reviewers for important comments and suggestions. WesternGeco provided the Gulf of Mexico data, and Smaart JV the Pluto synthetic-model dataset.

REFERENCES

Biondi, B., and W. Symes, 2004, Angle-domain common-image gathers for migration velocity analysis by wavefield-continuation imaging: Geophysics, **69**, 1283–1298.

Biondi, B., T. Tisserant, and W. Symes, 2003, Wavefield-continuation angle-domain common-image gathers for migration velocity analysis: 73rd Annual International Meeting, SEG, Expanded Abstracts, 2104–2107.

Bishop, K., P. Keliher, J. Paffenholz, D. Stoughton, S. Michell, R. Ergas, and M. Hadidi, 2001, Investigation of vendor demultiple technology for complex subsalt geology: 71st Annual International Meeting, SEG, Expanded Abstracts, 1273–1276.

de Bruin, C., C. Wapenaar, and A. Berkhout, 1990, Angle-dependent reflectivity by means of prestack migration: Geophysics, **55**, 1223–1234.

Duquet, B., and K. J. Marfurt, 1999, Filtering coherent noise during prestack depth migration: Geophysics, **64**, 1054–1066.

Foster, D. J., and C. C. Mosher, 1992, Suppression of multiple reflections using the Radon transform: Geophysics, **57**, 386–395.

Guitton, A., M. Brown, J. Rickett, and R. Clapp, 2001, Multiple attenuation using a t-x pattern based subtraction method: 71st Annual International Meeting, SEG, Expanded Abstracts, 1305–1308.

Guitton, A., and W. Symes, 2003, Robust inversion of seismic data using the huber norm: Geophysics, **68**, 1310–1319.

Hugonnet, P., P. Herrmann, and C. Ribeiro, 2001, High Resolution Radon—a Review: 63rd Meeting, European Association of Geoscientists and Engineers, Session: IM–2.

Kabir, M. M. N., and K. J. Marfurt, 1999, Toward true amplitude multiple removal: The Leading Edge, **18**, 66–73.

Kostov, C., 1990, Toeplitz structure in slant-stack inversion: 60th Annual International Meeting, SEG, Expanded Abstracts, 1618–1621.

Levin, S., and D. Johnston, 2001, A hybrid surface-related multiple attenuator: 71st Annual International Meeting, SEG, Expanded Abstracts, 1321–1324.

Miley, M., J. Paffenholz, K. Hall, and S. Michell, 2001, Optimizing surface-related multiple elimination on a synthetic subsalt data set: 71st Annual International Meeting, SEG, Expanded Abstracts, 1277–1280.

Mosher, C., and D. Foster, 2000, Common angle imaging conditions for prestack depth migration: 70th Annual International Meeting, SEG, Expanded Abstracts, 830–833.

Prucha, M., B. Biondi, and W. Symes, 1999, Angle-domain common-image gathers by wave-equation migration: 69th Annual International Meeting, SEG, Expanded Abstracts, 824–827.

Sacchi, M. D., and T. J. Ulrych, 1995, High-resolution velocity gathers and offset space reconstruction: Geophysics, **60**, 1169–1177.

Sava, P., and S. Fomel, 2003, Angle-domain common-image gathers by wavefield continuation methods: Geophysics, **68**, 1065–1074.

Stolk, C., and W. Symes, 2002, Artifacts in Kirchhoff common image gathers: 72nd Annual International Meeting, SEG, Expanded Abstracts, 1129–1132.

Thorson, J. R., and J. F. Claerbout, 1985, Velocity stack and slant stochastic inversion: Geophysics, **50**, 2727–2741.

van Dedem, E., and D. Verschuur, 2001, 3-D surface multiple prediction using sparse inversion: 71st Annual International Meeting, SEG, Expanded Abstracts, 1285–1288.

Verschuur, D. J., A. J. Berkhout, and C. P. A. Wapenaar, 1992, Adaptive surface-related multiple elimination: Geophysics, **57**, 1166–1177.

Weglein, A., and R. Stolt, 1999, Migration-inversion revisited: The Leading Edge, **18**, 950–952.